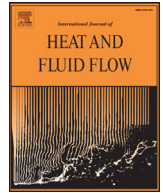




Contents lists available at ScienceDirect

## International Journal of Heat and Fluid Flow

journal homepage: [www.elsevier.com/locate/ijhff](http://www.elsevier.com/locate/ijhff)

# The combined effect of electric forces and confinement ratio on the bubble rising

A. Rahmat<sup>a,b</sup>, N. Tofighi<sup>a,b</sup>, M. Yildiz<sup>a,b,c,\*</sup>

<sup>a</sup>Faculty of Engineering and Natural Sciences, Sabanci University, Tuzla, 34956 Istanbul, Turkey

<sup>b</sup>Integrated Manufacturing Technologies Research and Application Center, Sabanci University, Tuzla, 34956, Istanbul, Turkey

<sup>c</sup>Sabancı University-Kordsa Global, Composite Technologies Center of Excellence, Istanbul Technology Development Zone, Sanayi Mah. Teknopark Blvd. No: 1/1B, Pendik, 34906 Istanbul, Turkey

## ARTICLE INFO

### Article history:

Received 7 September 2016

Revised 22 December 2016

Accepted 5 January 2017

Available online xxx

### Keywords:

Multiphase flows

Confinement ratio

Numerical simulations

VOF method

Bubble dynamics

Electrohydrodynamics (EHD)

## ABSTRACT

In this work, the combined effect of electrohydrodynamic forces and domain confinement on the formation of a toroidal bubble is numerically studied. The numerical scheme is the Volume of Fluid (VOF) method and the surface tension and electric forces are implemented using the Continuum Surface Force (CSF) and leaky dielectric models, respectively. It is found that both domain confinement and electric forces are influential on the formation of a toroidal bubble. For smaller confinement ratios, larger electric forces are required to pierce the bubble. Moreover, the influence of both electric forces and confinement ratio are presented and discussed for bubble vertical velocity, terminal Reynolds number, velocity streamlines and side-wall shear stress.

© 2017 Elsevier Inc. All rights reserved.

## 1. Introduction

The motion of a lighter fluid with a continuous interface in another heavier fluid due to the gravitational force is known as the bubble rising. In addition to numerous natural phenomena, there are plenty of industrial applications such as liquid separation and waste-water treatments (Takahashi et al., 1979; Al-Shamrani et al., 2002), nucleate pool boiling (Yoon et al., 2001) and chemical reactions (Pigeonneau, 2009) where the bubble rising is frequently observed. In most of these applications, the bubble rising is normally accompanied by the deformation of the bubble due to external, environmental and geometrical parameters. Numerous studies have been carried out to investigate the effect of various parameters on the regimes of bubble rising. Clift (Clift et al., 1978) reviewed the bubble rising and illustrated that the motion of the bubble can be categorized by three dimensionless numbers, namely the Reynolds, Morton, and Eotvos numbers which the later can also be referred to as the Bond number. He showed that in small Reynolds and Bond numbers, the bubble remains spherical, but increments of both Reynolds and Bond numbers yield different bubble regimes such as elliptical and spherical caps, as well as ellipsoidal and wobbling shapes. Further investigations (Chen et al., 1999; Bonometti

and Magnaudet, 2006; Han et al., 2010; Hua and Lou, 2007) revealed that bubbles may deform to a toroid under sufficiently large magnitudes of Reynolds and Bond numbers.

Chen et al. (1999) studied the bubble deformation and its rise for variations of Reynolds, Bond, density and viscosity ratios, and observed that the transition from an elliptical cap to a toroid is facilitated by means of a jet at the wake of the bubble. They concluded that such a transition occurs in density ratios of greater than 5, but the viscosity ratio does not have a significant effect on the bubble shape and velocity. They also realized that a toroidal bubble always travels slower than an elliptical or mushroom-shaped bubble. Bonometti and Magnaudet (2006) investigated the transition from a spherical cap to a toroidal bubble and realized that the transition takes place by means of two different scenarios. In the first scenario, they mentioned that for large Reynolds numbers, an upward liquid jet is driven by the hydrostatic pressure difference between the two poles of the bubble. If surface tension can not compete with the force due to the upward jet current, the bubble is pierced. The piercing occurs at the Bond number  $32 \leq Bo \leq 35$ . The piercing due to the second scenario occurs in the absence of surface tension force. If the viscous effects are not sufficiently strong to sustain the local pressure maximum at the bubble front, a toroidal bubble is formed. The second scenario is found to take place in Reynold number  $79 \leq Re \leq 84$ . Later, Hua and Lou (2007) numerically studied the bubble rising and reported that for constant magnitudes of Reynolds, Bond, density and viscosity

\* Corresponding author.

E-mail address: [meiyildiz@sabanciuniv.edu](mailto:meiyildiz@sabanciuniv.edu) (M. Yildiz).

ratios, a toroidal bubble is more likely to be formed when the bubble has an initial prolate shape compared to an initially oblate one. Nonetheless, these bubble regimes can also be affected by other parameters such as external forces and domain constraints.

The electrohydrodynamics (EHD), the imposition of electrical forces on fluid flow problems, is one of the means of manipulating flow regimes in bubble rising problems. Mählmann and Pappageorgiou (2009) studied the electrified bubble rising in a two-dimensional space for spherical and ellipsoidal rising regimes under the assumption of perfect dielectric model. They revealed that the bubble initially deforms to a prolate shape and later changes to an oblate shape performing "wobbly-like" oscillations. They also showed that the EHD effects increase the vertical rise velocity of the bubble. Wang et al. (2015) simulated the influence of EHD effects on bubble rising and showed that increments of the electric field strength has a direct relationship with the deformation of bubble. They also illustrated that further increments of electric field lead to the formation of a toroidal shape.

Also, the domain constraints have a significant effect on the bubble morphology. Mukundakrishnan et al. (2007) investigated the effect of domain confinement in a two-dimensional axisymmetric geometry on the bubble rising. They realized that the vertical and horizontal confinements are important when the domain height and width are smaller than 8 and 3 times of the bubble diameter, respectively. Recently, Kumar and Vanka (2015) studied the effect of domain confinement on bubble dynamics in a square duct for Bond number ranges of 1 – 100 and three confinement ratios and realized that for Bond number of 1, the bubble does not deform and corresponding aspect ratios (the ratio of vertical bubble diameter over its horizontal diameter) are independent of confinement and Reynolds number. For higher Bond numbers, however, the deformation is significant and the aspect ratio increases by incrementing both Bond number and confinement ratio. Nevertheless, the combined effect of the external electric forces on the bubble dynamics during its rising in a confined domain and possible influence of the EHD effects on the on the formation of a toroidal bubble has not been studied yet.

In this paper, the combined effect of external electric force and confinement ratio on the formation of a toroidal bubble is numerically investigated. In Section 2, the governing equations and dimensionless parameters are presented. In Section 3, the computational domain and relevant boundary conditions are introduced. Moreover in Section 3, the numerical tool is validated by comparing the results with some of those available in the literature, and the dependency of the results with respect to the grid resolution is tested. In Section 4, the results are provided and the combined effect of electrical Capillary and confinement ratio on the formation of a toroidal bubble is discussed. Finally, the concluding remarks are presented in Section 5.

## 2. Governing equations and numerical scheme

Equations governing an incompressible flow may be written as

$$\nabla \cdot \mathbf{u} = 0, \quad (1)$$

$$\rho \frac{D\mathbf{u}}{Dt} = -\nabla p + \frac{1}{Re} \nabla \cdot \mathbf{T} + \frac{1}{Bo} \mathbf{f}_{(s)} + \frac{1}{Eg} \mathbf{f}_{(e)}, \quad (2)$$

where  $\mathbf{u}$  is the velocity vector,  $p$  is pressure,  $\rho$  is density,  $t$  is time and  $D/Dt = \partial/\partial t + \mathbf{u} \cdot \nabla$  represents the material time derivative. In this study, normal letters indicate scalar quantities and bold letters represent vectors and tensors. Here,  $\mathbf{T}$  is the viscous stress tensor,

$$\mathbf{T} = \mu [\nabla \mathbf{u} + (\nabla \mathbf{u})^\dagger], \quad (3)$$

where  $\mu$  denotes viscosity and superscript  $\dagger$  represents the transpose operation. Local surface tension force is expressed as an

equivalent volumetric force according to the continuum surface (CSF) method (Brackbill et al., 1992),

$$\mathbf{f}_{(s)} = \gamma \kappa \hat{\mathbf{n}} \delta. \quad (4)$$

Here, surface tension coefficient,  $\gamma$ , is taken to be constant while  $\kappa$  represents interface curvature,  $-\nabla \cdot \hat{\mathbf{n}}$ , where  $\hat{\mathbf{n}}$  is unit surface normal vector.  $\mathbf{f}_{(e)}$  is the electric force vector defined as (Saville, 1997)

$$\mathbf{f}_{(e)} = -\frac{1}{2} \mathbf{E} \cdot \nabla \varepsilon + q^v \mathbf{E}. \quad (5)$$

In the above equation,  $\varepsilon$  denotes electric permittivity,  $q^v$  is the volume charge density near the interface while  $\mathbf{E}$  is the electric field vector. Assuming small dynamic currents and neglecting magnetic induction effects, the electric field is irrotational Hua et al. (2008) and may be represented by gradient of an electric potential  $\phi$ ,  $\mathbf{E} = -\nabla \phi$ . In the above equation, the electrostrictive force vanishes due to the fact that the system is assumed to be incompressible, thus the electric permittivity does not vary with respect to the fluid density (Eringen and Maugin, 2012). Further assumption of fast electric relaxation time compared to viscous relaxation time leads to the following relations for electric potential and charge density

$$\nabla \cdot (\sigma \nabla \phi) = 0, \quad (6)$$

$$q^v = \nabla \cdot (\varepsilon \nabla \phi), \quad (7)$$

where  $\sigma$  is the electrical conductivity.

Dimensionless values are formed using the following scales

$$\mathbf{r} = \mathbf{r}^+/d, \quad \mathbf{z} = \mathbf{z}^+/d, \quad \rho = \rho^+/\rho_f, \quad \mu = \mu^+/\mu_f, \quad \mathbf{u} = \mathbf{u}^+/\sqrt{gd}, \\ t = t^+ \sqrt{g/d}, \quad \mathbf{E} = \mathbf{E}^+/E_\infty, \quad p = (p^+ - \rho_f \mathbf{g} \cdot \mathbf{x}^+)/\rho_f g d, \\ D = \rho_b/\rho_f, \quad \nu = \mu_b/\mu_f, \quad \mathcal{P} = \varepsilon_b/\varepsilon_f, \quad C = \sigma_b/\sigma_f, \quad (8)$$

leading to Reynolds, Bond, Electro-gravitational and Electro-capillary numbers defined as

$$Re = \frac{\rho_f \sqrt{gd}^3}{\mu_f}, \quad Bo = \frac{\rho_f g d^2}{\gamma}, \quad Eg = \frac{\rho_f g d}{\varepsilon_f E_\infty^2}, \quad Ec = \frac{Bo}{Eg} = \frac{\varepsilon_f E_\infty^2 d}{\gamma}. \quad (9)$$

Here  $d$  is the bubble diameter,  $E_\infty$  is the undisturbed electric field intensity and  $g$  is the gravitational acceleration. A plus sign marks dimensional variables whereas subscripts  $\square_b$  and  $\square_f$  denote bubble and surrounding fluid phases, respectively.

In the Volume of Fluid (VOF) method, the volume fraction  $\alpha$  is calculated by solving an evolution equation as,

$$\frac{\partial \alpha}{\partial t} + \mathbf{u} \cdot \nabla \alpha = 0, \quad (10)$$

and fluid properties are smoothed on the interface by,

$$\xi = \alpha \xi_b + (1 - \alpha) \xi_f, \quad (11)$$

where  $\xi$  can be any physical fluid property such as density, viscosity, electrical conductivity or permittivity whichever is appropriate.

In this paper, the finite volume method is used to discretize the continuity and momentum equations. The momentum equation (Eq. 2) is solved by a second-order upwind formulation both in time and space. The PRESTO! method is employed to calculate the pressure field, and the pressure and velocity fields are coupled using the SIMPLE scheme.

The commercial ANSYS Fluent software is used to solve the relevant governing equations together with the associated boundary conditions. In addition to the continuity and momentum equations, a Laplace equation needs to be solved to obtain the electric field (Eq. 6) in the domain. This has been carried out using a User Defined Function (UDF). Then, the electric field is evaluated as the

Download English Version:

<https://daneshyari.com/en/article/4993140>

Download Persian Version:

<https://daneshyari.com/article/4993140>

[Daneshyari.com](https://daneshyari.com)